INDIAN JOURNAL OF SCIENCE AND TECHNOLOGY

RESEARCH ARTICLE



OPEN ACCESS

**Received:** 20-09-2024

**Accepted:** 28-10-2024

**Published:** 30-11-2024

**Citation:** Sammy K, Singh S (2024) Homoclinic Orbit of Kerr Black Holes. Indian Journal of Science and Technology 17(44): 4582-4589. https://doi.org/10.17485/IJST/v17i44.3029

* **Corresponding author**.

**Funding:** None

**Competing Interests:** None



Published By Indian Society for Education and Environment (iSee)

**ISSN**
Print: 0974-6846
Electronic: 0974-5645

# Homoclinic Orbit of Kerr Black Holes

**Kumari Sammy[1], Sumita Singh[2]***

**1** Research Scholar, Department of Physics, Patna University, Patna, 800005, Bihar, India
**2** University Professor, Department of Physics, Patna University, Patna, 800005, Bihar, India

## Abstract

**Objective:** This study investigates the effective potential and homoclinic orbit near the Kerr metric system of black holes. It also examines the graphical relationship between effective potential and radial momentum with distance from black holes. **Methods:** The motion of a test particle near the Kerr metric has been analyzed using the Euler Lagrangian and action-angle variable methods. The graphical analysis in this study was performed with Mathematica software. **Findings:** An expression for effective potential and radial momentum has been evaluated. It has been shown that homoclinic orbits exist near the Kerr metric. This study presents a graphical analysis of the effective potential of test particles in Kerr metric black holes with different polar angle and spin. Homoclinic orbits are visually represented in this paper with the help of graphical analysis. **Novelty:** A physical interpretation of the effective potential and geodesic motion near Kerr metric black holes has been obtained. These results provide a valuable tool for detecting chaos in the Kerr metric of black holes. In this paper, we have shown the changes in the motion of a particle when it comes near the horizon of Kerr black holes. Indicators of chaos can give an insight into understanding the black hole phenomena. Graphical analysis offers a visual understanding of the motion of test particles near the Kerr metric geometry of Black holes.

**Keywords:** Black holes; Kerr Metric; Melnikov method; Chaos; Effective Potential; Homoclinic Orbit

## 1 Introduction

Theoretically, Black holes are solutions to Einstein's theory of relativity. A recent series of papers by L. Polcar[(1)] et.al. (2019) used the Melnikov method to detect the homoclinic orbit of the Schwarzschild black hole simulated by the Nowak-Wagoner pseudo-potential and encircled by the Bach-Weyl ring or the inverted first Morgan-Morgan disc, and the extreme Reissner-Nordstrom black hole encircled by the extremely charged, Majumdar-Papapetrou ring. Xiaobo Guo[(2)] et. al (2020) briefly described the chaotic motion around a black hole under minimal length effects of the Schwarzschild metric as a special case. Yu-Qi Lei[(3)] et.al (2021) derived the chaotic behavior of particle motion in black holes with quasi-topological electromagnetism. These papers give us an idea of how we can describe homoclinic orbit near the Kerr metric of black holes.

Chen-Yu Wang [4] et.al (2022) derived the null and time-like geodesic for Kerr-Newman black holes. Yi Ting Li [5] et. al. (2023) described the homoclinic orbits of Kerr-Newman Black holes using radial potential with varying azimuthal momentum. In this paper, they derived the solution for the non-equatorial orbit in Kerr-Newman black holes. A. S Alam [6] et. al. (2024) investigated the spherical orbits around the Kerr-Newman and Ghosh black holes. Xuan Zhou [7] et.al(2021) employed the equation of motion for test particle coupling to the Chern-Simon invariant in Kerr metric black hole spacetime. Pankaj Sheoran [8] et.al (2018) used the scalar-tensor–gravity theory to derive the geodesic motion of test particles around Kerr-MOG spacetime. Prerna Rana [9] et.al.(2019) described the trajectories around a Kerr black hole by using the transformation of radial distance from black holes. In this paper authors derived the relation between energy and angular momentum of the particle and sketched the spherical bound orbits, homoclinic orbits, and zoom-whirl orbits using the parameters eccentricity, inverse-latus rectum, spin, and Carter's constant. Bijay Kumar Sharma [10] (2024) used experimental data of super Massive black holes in NG1365 to derive effective potential, stable, and unstable circular orbit of Kerr metric.

We found a noticeable gap in the literature. No paper has shown the geodesic motion of test particles near Kerr black holes with changing polar angles. Most of the papers only evaluated the effective potential of test particles around Kerr metric black holes but here we described the effective potential and radial momentum for test particles around black holes with different polar angles. Graphical analysis of effective potential as a function of radial distance determines the stability criteria for orbits. These concepts lead to drawing the homoclinic orbit for Kerr metric black holes. Further, our findings provide valuable insight into the chaotic behavior of Kerr black holes.

This paper is organized as follows: in section 2 we have described the equations of motion for test particles moving around Kerr metric black holes and we have evaluated the effective potential and radial momentum for Kerr metrics of black holes. Section 3 is dedicated to results and discussions. Section 4 is dedicated to the conclusion and future application of our work. Section 5 provides acknowledgments of this paper. The last section 6 references.

## 2 Tracing of homoclinic orbits using Kerr metric

Homoclinic orbit is a (closed) trajectory that has a hyperbolic (saddle) fixed point of the respective flow as both its past and future asymptote. Along such an orbit, the tangent bundle of the configuration manifold splits into stable and unstable invariant sub-bundles, spanning sub-manifolds in which the flow is contracting and expanding, respectively (thus saddle point). In the unperturbed system, these sub-manifolds intersect "longitudinally" and thus coincide along the Homoclinic orbit. If the perturbation deforms them in such a way that they start to intersect transversally along that orbit, it is a signature that the orbit has "broken up" into a chaotic layer (so-called Smale-Birkhoff Homoclinic theorem). When a particle moves around the black holes it creates the homoclinic orbit. Homoclinic orbit around the black holes gives first indicator of the chaotic behavior of black holes. Moser and Smale-Birkhoff rely on the fact that the flow possesses a hyperbolic periodic point and the stable and unstable manifolds of this point intersect transversely. If these conditions are met, then there exists an invariant Cantor set that is topologically conjugate to a shift map implying that the flow is chaotic [11]. In this paper, we have obtained the expression of effective potential and drawn the homoclinic orbit for the Kerr metric black hole.

### 2.1 Methodology

While describing Hamiltonian trajectory around black holes we have considered a relativistic particle moving in a x space-time described by the metric $g_{ab}$. The world-line of a particle will be denoted by $x^a(s)$ and its mass by $\mu$. The canonical conjugate momentum to $x^a$ is

$$P_a = \mu g_{ab} \dot{x^b} \tag{1}$$

and

$$\dot{x^b} = \frac{dx^b}{ds} \tag{2}$$

The motion of the particle can be obtained from the action [11] [12] [13]

$$S[x] = \frac{\mu}{2} \int g_{ab}\, \dot{x^a} \dot{x^b} ds \tag{3}$$

This action is not a reparameterization invariant but is made simple for our purposes. **s** is the proper time along the world line. The canonical conjugate momentum satisfy the mass shell constraint.

$$g^{ab} P_a P_b = -\mu^2 \tag{4}$$

The Hamiltonian of the system is given by

$$H = \frac{1}{2\mu} g^{ab} P_a P_b \tag{5}$$

We take the metric of different Kerr black holes to find the homoclinic path of black holes.

$$ds^2 = -\left(1 - \frac{2Mr}{\Sigma}\right) dt^2 - \frac{4aMrsin^2\theta}{\Sigma} dtd\emptyset + \frac{\Sigma}{\Delta} dr^2 + d\theta^2 + (r^2 + a^2 + \frac{2a^2Mrsin^2\theta}{\Sigma}) sin^2\theta d\emptyset^2 \tag{6}$$

Where symbols stand for

$\triangle$=$r^2 + a^2 - 2Mr,\ \Sigma = r^2 + a^2cos^2\theta$, $a$=J/M, t=time coordinate, $\theta$=Polar angle, $\phi$=Azimuthal angle , r=Radial distance from black hole ($r\ is\ multiple\ of\ R_{sch}$), $a$ = Spin parameter of the black hole, M=Mass of the black hole(M is multiple of Sun mass).

For $\theta = \pi/2,\ d\theta = 0,\ \Sigma = r^2$ Kerr metric becomes

$$ds^2 = -\left(1 - \frac{2M}{r}\right) dt^2 - \frac{4aM}{r} dtd\emptyset + \frac{r^2}{\Delta} dr^2 + (r^2 + a^2 + \frac{2a^2M}{r}) d\emptyset^2 \tag{7}$$

The Lagrangian for Kerr given system is

$$2L == -\left(1 - \frac{2M}{r}\right) \mu \dot{t}^2 - \frac{4aM}{r} \mu \dot{t}\dot{\emptyset} + \frac{r^2}{\Delta} \mu \dot{r}^2 + (r^2 + a^2 + \frac{2a^2M}{r}) \mu \dot{\emptyset}^2 \tag{8}$$

where,

$$\dot{t} = \frac{dt}{ds}$$
$$\dot{r} = \frac{dr}{ds}$$
$$\dot{\emptyset} = \frac{d\emptyset}{ds}$$

$We\,have$ generalized momenta for a given system is

$$E = -P_t = \mu \left(1 - \frac{2M}{r}\right) \dot{t} - \frac{4aM}{r} \mu \dot{\emptyset} \tag{9}$$

$$L = P_\phi = -\frac{2aM}{r} \mu \dot{t} + (r^2 + a^2 + \frac{2a^2M}{r}) \mu \dot{\emptyset} \tag{10}$$

$$P_r = \frac{\mu r^2}{\Delta} \dot{r} \tag{11}$$

From Equation (9) and Equation (10), we get

$$\dot{\emptyset} = \frac{1}{\mu \triangle} \left[ L \left(1 - \frac{2M}{r}\right) + \frac{2aME}{r} \right] \tag{12}$$

$$\dot{t} = \frac{1}{\mu \triangle} \left[ E \left( r^2 + a^2 + \frac{2a^2M}{r} \right) - \frac{2aML}{r} \right] \tag{13}$$

Hamiltonian for a given system is

$$H = P_t \dot{t} + P_\emptyset \dot{\emptyset} + P_r\ \dot{r} - L \tag{14}$$

Using Equations (9), (10), (11), (12) and (13) and Equation (5) we get

$$2H = -E\dot{t} + L\dot{\emptyset} + \frac{\mu r^2}{\triangle} \dot{r}^2 = Constant \tag{15}$$

Inserting the value of $\dot{t}$, $\dot{\emptyset}$ and $\dot{r}$ in Equation (15) and using Equation (4) and Equation (5) we get the equation of motion for a given system

$$\mu^2\left(\frac{dr}{ds}\right)^2-\frac{\left(a^2E^2-L^2\right)}{r^2}-\frac{2M\left(a^2E^2+L^2-2aEL\right)}{r^3}+\frac{a^2\mu^2}{r^2}-\frac{2M\mu^2}{r}=E^2-\mu^2 \tag{16}$$

We know that the general equation can be written as

$$\mu^2\left(\frac{dx}{d\phi}\right)^2+V_{effective}\left(x\right)=E^2-\mu^2 \tag{17}$$

For the existence of a Homoclinic orbit, the effective potential in the above equation V(x) has an unstable equilibrium point. Potential V(x) has extremum at real values of x.

From Equation (16) and Equation (17) we get the effective potential for test particle trajectory for the Kerr geometry system as

$$V_{effective}=-\frac{2M\mu^2}{r}-\frac{\left(a^2E^2-L^2-a^2\mu^2\right)}{r^2}-\frac{2M\left(aE-L\right)^2}{r^3} \tag{18}$$

**Using Equation (16), Equation (11) becomes**

$$P_r=\frac{\mu r^2}{\Delta}\dot{r}=\pm\frac{r^2}{\Delta}\sqrt{E^2-\mu^2+\frac{2M\mu^2}{r}+\frac{\left(a^2E^2-L^2-a^2\mu^2\right)}{r^2}+\frac{2M\left(aE-L\right)^2}{r^3}} \tag{19}$$

$P_r =$ **Radial momentum.**

**Similarly, we take** $\theta=\pi/4,\ d\theta=0,\ \Sigma=r^2+\frac{a^2}{2}$ Kerr metric becomes

$$ds^2=-\left(1-\frac{4Mr}{2r^2+a^2}\right)dt^2-\frac{4aMr}{2r^2+a^2}dtd\emptyset+\frac{2r^2+a^2}{2\Delta}dr^2+(r^2+a^2+\frac{2a^2Mr}{2r^2+a^2})\frac{1}{2}d\emptyset^2 \tag{20}$$

$$V_{effective}=\frac{2r^2}{2r^2+a^2}\left[2\frac{L^2}{r^2}+\left(\frac{\mu^2a^2}{r^2}-\frac{E^2a^2}{r^2}\right)-\frac{2M\mu^2}{r}-\frac{2M(aE-2L)^2}{r(2r^2+a^2)}\right] \tag{21}$$

$$P_r=\frac{\mu(2r^2+a^2)}{2\Delta}\dot{r}=\pm\frac{(2r^2+a^2)}{2\Delta}\sqrt{\frac{2r^2}{(2r^2+a^2)}\left[E^2-\mu^2-2\frac{L^2}{r^2}+\left(\frac{E^2a^2}{r^2}-\frac{\mu^2a^2}{r^2}\right)+\frac{2M\mu^2}{r}+\frac{2M(aE-2L)^2}{r(2r^2+a^2)}\right]} \tag{22}$$

**Similarly, we take** $\theta=\pi/6,\ d\theta=0,\ \Sigma=r^2+\frac{3a^2}{4}$ Kerr metric becomes

$$ds^2=-\left(1-\frac{8Mr}{4r^2+3a^2}\right)dt^2-\frac{4aMr}{4r^2+3a^2}dtd\emptyset+\frac{4r^2+3a^2}{4\Delta}dr^2+\left(\frac{r^2}{4}+\frac{a^2}{4}+\frac{a^2Mr}{2(4r^2+3a^2)}\right)d\emptyset^2 \tag{23}$$

$$V_{effective}=\frac{4r^2}{4r^2+3a^2}\left[4\frac{L^2}{r^2}+\left(\frac{\mu^2a^2}{r^2}-\frac{E^2a^2}{r^2}\right)-\frac{2M\mu^2}{r}-\frac{2M(aE-4L)^2}{r(4r^2+3a^2)}\right] \tag{24}$$

$$P_r=\frac{\mu(4r^2+3a^2)}{4\Delta}\dot{r}=\pm\frac{(4r^2+3a^2)}{4\Delta}\sqrt{\frac{4r^2}{(4r^2+3a^2)}\left[E^2-\mu^2-4\frac{L^2}{r^2}+\left(\frac{E^2a^2}{r^2}-\frac{\mu^2a^2}{r^2}\right)+\frac{2M\mu^2}{r}+\frac{2M(aE-4L)^2}{r(4r^2+3a^2)}\right]} \tag{25}$$

## 3 Results and Discussions

In this paper, we have studied the geodesic motion near Kerr metric black holes with standard metric. We have applied the Euler-Lagrangian and Action angle variables methods to find the expressions for effective potential ($V_{effective}$) and radial momentum ($P_r$) of a given system. A range of significant outcomes are highlighted below.

We have evaluated the expression for effective potential and radial momentum for test particle trajectory around Kerr metric black holes. We have obtained a graph between effective potential and radial distance from the Kerr metric black holes for different polar angle and mass of Kerr black holes.

Here, we have assumed some values for graphical analysis of effective potential. We know that existence of event horizon conditions for Kerr black holes $M^2 \geq a^2$.We take M=1, $a$ =0.5, 0.9, $\mu = 10^{-6}$ and $L = 3.78 \times 10^{-6}$. Using these assumptions and expressions obtained for effective potential correspond to $\theta = \frac{\pi}{2}, \frac{\pi}{4}, \frac{\pi}{6}$ we obtained the energy per unit mass (E) for unstable orbit near Kerr black holes. For M=1, $a$ =0.5, 0.9 and $\theta = \frac{\pi}{2}$ , the value of $E = 0.302217 \times 10^{-6}$, $0.278572 \times 10^{-6}$. Similarly, M=1, , $a$ =0.5, 0.9 and $\theta = \frac{\pi}{4}$ , the value of $E = 8.85376 \times 10^{-6}$, $2.27231 \times 10^{-6}$ and M=1, $a$ =0.5, 0.9 and $\theta = \frac{\pi}{6}$ , the value of $E = 11.0679 \times 10^{-6}$, $3.18408 \times 10^{-6}$.

Using above findings and Equations (18) and (21) and Equation (24) we have depicted **Figure 1 (a) to Figure 6 (a)**. These Figures present the stable and unstable point for effective potential of test particle trajectory around Kerr metric black holes. The effective potential's equilibrium configuration are presented in **Figure 1(a) and Figure 2 (a)** , which exhibits an unstable equilibrium at $r = 3.64329R_{sch}$ ($r\ is\ multiple\ of\ Schwarzschild\ radius\ R_{sch}$)for $\theta = \frac{\pi}{2}, M = 1, a = 0.5$ and $r = 3.18176R_{sch}$ for $\theta = \frac{\pi}{2}, M = 1, a = 0.9$ , where as stable equilibrium arise at $r = 10.0022R_{sch}(\theta = \frac{\pi}{2}, M = 1, a = 0.5)$ and $r = 11.0029R_{sch}(\theta = \frac{\pi}{2}, M = 1, a = 0.9)$. Similarly, the effective potential plot in **Figure 3 (a)** and **Figure 4 (a)** demonstrates unstable equilibrium at $r = -0.16505R_{sch}$ for $\theta = \frac{\pi}{4}, M = 1, a = 0.5$, and $r = -0.259731R_{sch}$ for $\theta = \frac{\pi}{4}, M = 1, a = 0.9$, where as stable equilibrium arise at $r = 0.28R_{sch}(\theta = \frac{\pi}{4}, M = 1, a = 0.5)$ and $r = 0.6767R_{sch}(\theta = \frac{\pi}{4}, M = 1, a = 0.9)$. In the same way **Figure 5 (a)** and **Figure 6 (a)** also exhibits an unstable equilibrium at $r = 2.8R_{sch}$ for $\theta = \frac{\pi}{6}, M = 1, a = 0.5$ and $r = 1.87\ R_{sch}$ for $\theta = \frac{\pi}{6}, M = 1, a = 0.9$, whereas stable equilibrium arise at $r = 20R_{sch}(\theta = \frac{\pi}{6}, M = 1, a = 0.5)$ and $r = 20R_{sch}(\theta = \frac{\pi}{6}, M = 1, a = 0.9)$. At these values of radial distance (r) from Kerr black holes effective potentials are unstable and stable equilibrium. Unstable equilibrium leads to homoclinic orbit of Kerr black holes.

Bijay Kumar Sharma [10] (2024) derived similar figure of Schwarzschild and Kerr metric effective potential for specific super Massive black holes in NG1365. In this paper he used experimental data to derive effective potential, stable and unstable circular orbit of Kerr metric. Prerna [9] et.al (2019) has derived the expression for effective potential using new analytic solutions of non-equatorial eccentric bound trajectories. In this paper authors are using only general condition of polar angle but here we take some special case of polar angle to derive the effective potential of test particle around Kerr metric black holes.

Radial momentum for moving test particle near black holes are given in Equations (19) and (22) and Equation (25). With the help of these equations we have evaluated the radial momentum of Kerr metric for different value of $\theta$. We have also plotted the graphs between radial momentum ($P_r$) and radius(r) of black holes. Here, we take same assumptions and and value of E for graphical analysis of homoclinic orbit in phase space correspond to M=1, $a = 0.5, 0.9$ and $\theta = \frac{\pi}{2}, \frac{\pi}{4}, \frac{\pi}{6}$.

**Figure 1(b) to Figure 6 (b)** present the homoclinic orbit of test particle near Kerr black holes. Saddle points for trajectories are identified from these graphical analyses. **Figure 1(b), Figure 3 (b) and Figure 5 (b)** reveal saddle points at radial distances $r = 1.1646R_{sch}$, $r = -0.5378R_{sch}$ and $r = -0.873408R_{sch}$ for the parameters $M = 1, a = 0.5\ and\ \theta = \frac{\pi}{2}, \frac{\pi}{4}, \frac{\pi}{6}$. In the same way **Figure 2 (b), Figure 4 (b) and Figure 6 (b)** also exhibits the saddle points at $r = 1.356R_{sch}$, $r = -3.145R_{sch}$ and $r = -2.8281R_{sch}$ for the parameters $M = 1, a = 0.9\ and\ \theta = \frac{\pi}{2}, \frac{\pi}{4}, \frac{\pi}{6}$. \

Soyeon Jeong [14] et.al. obtained homoclinic orbit around black hole with anistropic matter fields. In this paper authors obtained trajectory of the particle near Schwarzschild and Resinner Nordstorm black holes that correspond to unstable local maximum of the effective potential.Similarly our studies also show that the homoclinic orbit obtained with unstable effective potential.Here we also evaluated the radial distance for unstable and stable orbit correspond to different polar angles and mass of Kerr black holes. P.A.Gonzalez [15] et.al. described the geodesic motion and orbits for Schwarzschild and Reissner black holes in five dimesions. So we can say that the our findings are new in case of Kerr black holes.No paper described the geodesic motion of test particle near Kerr black holes with different polar angles.In this study we obtained homoclinic orbit,stable and unstable radial distance for effective potential of test particle around Kerr black holes with different polar angles.

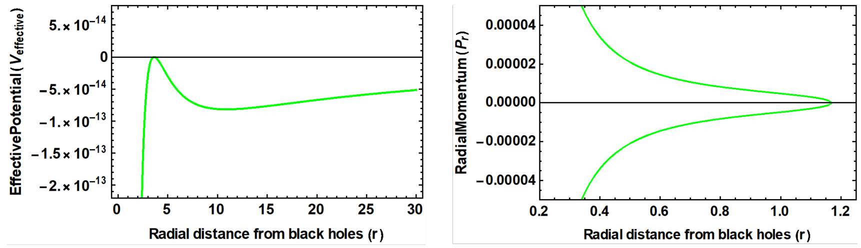


**Fig 1. (a) Plot of Effective potential at $\pi/2$ with energy E=0.302217 x $10^{-6}$ (b) Plot of Homoclinic orbit in phase space for $\pi/2$ with energy E=0.302217 x $10^{-6}$**

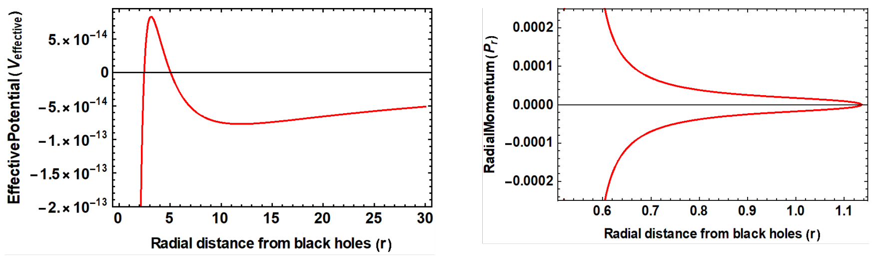


**Fig 2. (a) Plot of Effective potential at $\pi/2$ with energy E=0.278572 x $10^{-6}$ (b) Plot of Homoclinic orbit in phase space for $\pi/2$ with energy E=0.278572 x $10^{-6}$**

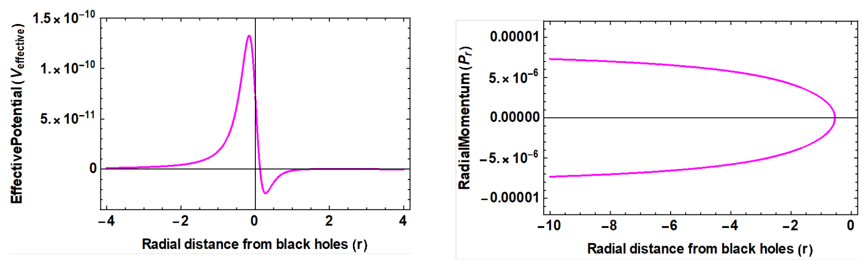


**Fig 3. (a) Plot of Effective potential at $\pi/4$ with energy E=8.85376 x $10^{-6}$ (b) Plot of Homoclinic orbit in phase space for $\pi/4$ with energy E=8.85376 x $10^{-6}$**

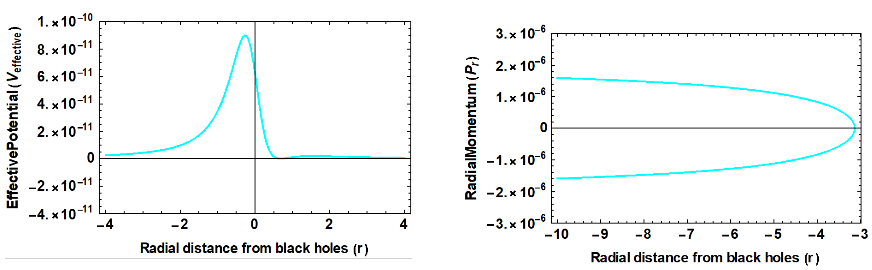


**Fig 4. (a) Plot of Effective potential at $\pi/4$ with energy E=2.27231 x $10^{-6}$ (b) Plot of Homoclinic orbit in phase space for $\pi/4$ with energy E=2.27231 x $10^{-6}$**

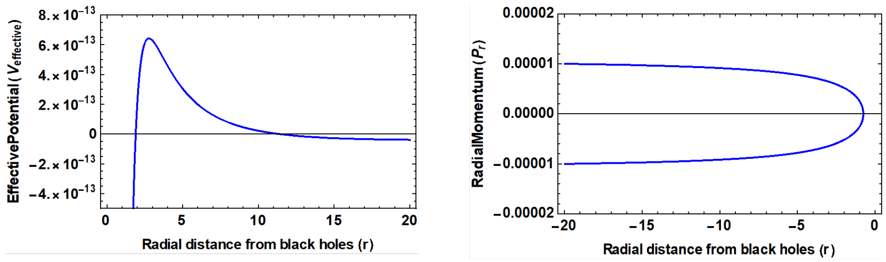


**Fig 5. (a) Plot of Effective potential at $\pi/6$ with energy E=11.069 x 10$^{-6}$ (b) Plot of Homoclinic orbit in phase space for $\pi/6$ with energy E=11.069 x 10$^{-6}$**

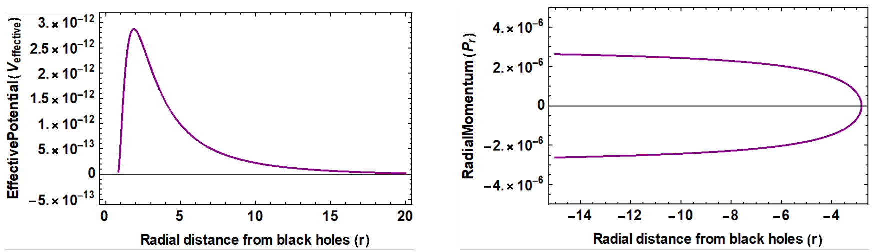


**Fig 6. (a) Plot of Effective potential at $\pi/6$ with energy E=3.18408 x 10$^{-6}$ (b) Plot of Homoclinic orbit in phase space for $\pi/6$ with energy E=3.18408 x 10$^{-6}$**

## 4 Conclusions

This study has evaluated effective potential and radial momentum for test particle near Kerr black holes at different polar angles. Our solution, using the semi-classical method provides a simple relation between effective potential, radial momentum with radial distance from Kerr black holes. Radial momentum plotting shows that intersection points of homoclinic orbit vary with spin parameter and polar angle. The geodesic motion of a test particle around a Kerr black hole is examined in this research. In this analysis we get the stable and unstable radial distance from black holes correspond to the effective potential of test particle near Kerr black holes. These radial distances very useful to determine trajectory of motion of test particle near Kerr metric black holes. The orbital nature of test particle near Kerr black hole has also been determined. Homoclinic orbit is useful to find the nonlinear behavior of black holes physics. Our findings can be applied to determine the chaotic indicator for celestial objects.

### Acknowledgment

The authors are thankful to the Department of Physics, Patna University and IISER (IAGRG-32) Kolkata, and to Prof. Vijay A. Singh for fruitful discussion.

## References

1) Polcar L, Semerak O. Free motion around black holes with discs or rings: between integerability and chaos-VI .The Melnikov method. *Physical Rev D* . 2019;100. Available from: https://doi.org/10.1103/PhysRevD.100.103013.
2) Xiaobo G, Liang K, Mu BE. Chaotic motion around a black hole under minimal length effects. *Eur Phys JC*. 2020;80:745–745. Available from: https://doi.org/10.1140/epjc/s10052-020-8335-6.
3) Yu-Qi L, Hui GX, Cheg R. Chaos of particle motion near a black hole with quasitopological electromagnetism. *Physical Rev D*. 2021;104:46020–46020. Available from: https://journals.aps.org/prd/references/10.1103/PhysRevD.104.046020.
4) Wang CY, Lee DS, Lin CY. Null and timelike geodesics in the Kerr-Newman black hole exterior. *Phys Rev D*. 2022;106:84048–84048. Available from: https://doi.org/10.1103/PhysRevD.106.084048.
5) Li YT, Wang CY, Lee DS, Lin CY. Homoclinic orbits in Kerr-Newman black holes. *Physical Review D*. 2023;108:44010–44010. Available from: https://journals.aps.org/prd/abstract/10.1103/PhysRevD.108.044010.
6) Alam AS, Andaru LC, Jayawiguna BN. Spherical orbits around Kerr-Newman and Ghosh black holes. *Gen Relativ Gravit*. 2024;56:79–79. Available from: https://doi.org/10.1007/s10714-024-03264-2.
7) Zhou X, Chen S, Jing J. Chaotic motion of scalar particle coupling to Chern-Simons invariant in Kerr black hole spacetime. *Eur Phys J C*. 2021;81:233–233. Available from: https://doi.org/10.1140/epjc/s10052-021-09042-7.
8) Sheoran P, Herrera-Aguilar A, Nucamendi U. Mass and spin of a Kerr black hole in modified gravity and a test of the Kerr black hole hypothesis. *Phys Rev D*. 2018;97:124049–124049. Available from: https://doi.org/10.1103/PhysRevD.97.124049.

9) Rana P, Mangalam A. Astrophysically relevant bound trajectories around a Kerr black hole. *Classical and Quantum Gravity*. 2019;36(4). Available from: https://doi.org/10.1088/1361-6382/ab004c.
10) Sharma BK. Correspondence of Concept of Circular Orbits in Schwarzschild Metric and Kerr Metric to those in Tidally Evolving Binaries in Weak Gravitational Regime and its Application in Determination of Spin of Supermassive Black Hole. *Journal of Mathematical Techniques and Computational Mathematics*. 2024;3(7):1–22. Available from: https://doi.org/10.33140/JMTCM.03.07.01.
11) Bombelli L, Calzetta E. Chaos around a black hole. *Classical and Quantum Gravity*. 1992;9. Available from: https://doi.org/10.1088/0264-9381/9/12/004.
12) Chandrasekhar S. The mathematical theory of black holes. Oxford. Clarendon Press. 1983. Available from: https://global.oup.com/academic/product/the-mathematical-theory-of-black-holes-9780198503705.
13) Misner CW, Thorne KS, Wheeler JA. Gravitation. New York, New York. Freeman. 1973.
14) Jeong S, Lee BH, Lee H, Lee W. Homoclinic orbit and the violation of chaos bound around a black hole with anisotropic matter fields. *Physical ReviewD*. 2023;107:104037–104037. Available from: https://doi.org/10.1103/PhysRevD.107.104037.
15) Gonzalez PA, Olivares M, Vasquez Y, Villanueva JR. Time like geodesic for five dimensional Schwarzschild and Reissner-Nordstrom anti-de Sitter black holes. *The European Physical Journal C*. 2023. Available from: https://doi.org/10.1140/epjc/s10052-023-12018-4.